Online-Journals.org

iJOE International Journal of Online and Biomedical Engineering

iJOE | eISSN: 2626-8493 | Vol. 19 No. 18 (2023) | OPEN ACCESS

https://doi.org/10.3991/ijoe.v19i18.43943

PAPER

Computer Vision-Based Approach for Automated Monitoring and Assessment of Gait Rehabilitation at Home

Safae Talaa(✉), Mohamed El Fezazi, Abdelilah Jilbab, My Hachem El yousfi Alaoui

Electronic Systems Sensors and Nanobiotechnology, National School of Arts and Crafts, Mohammed V University in Rabat, Rabat, Morocco

safae_talaa@um5.ac.ma

ABSTRACT

This study presents a markerless video-based human gait analysis system for automatic assessment of at-home rehabilitation. A marker-based MoCap system (Vicon) is used to evaluate the accuracy of the proposed approach. Additionally, a novel gait rehabilitation score based on the Dynamic Time Warping (DTW) algorithm is introduced, enabling quantification of rehabilitation progress. The accuracy of the proposed approach is assessed by comparing it to a marker-based MoCap system (Vicon), which is used to evaluate the proposed approach. This evaluation results in mean absolute errors (MAE) of 4.8° and 5.2° for the left knee, and 5.9° and 5.7° for the right knee, demonstrating an acceptable accuracy in knee angle measurements. The obtained scores effectively distinguish between normal and abnormal gait patterns. Subjects with normal gait exhibit scores around 97.5%, 98.8%, while those with abnormal gait display scores around 30%, 29%, respectively. Furthermore, a subject at an advanced stage of rehabilitation achieved a score of 65%. These scores provide valuable insights for patients, allowing them to assess their rehabilitation progress and distinguish between different levels of gait recovery. The proposed markerless approach demonstrates acceptable accuracy in measuring knee joint angles during a sagittal walk and provides a reliable rehabilitation score, making it a convenient and cost-effective alternative for automatic at-home rehabilitation monitoring.

KEYWORDS

gait analysis, pose estimation, knee angle, score rehabilitation

1 INTRODUCTION

Rehabilitation is a crucial aspect of healthcare to achieve universal health coverage. According to [1], approximately 2.41 billion people received rehabilitation for their health conditions in 2019, indicating a significant increase of 63% compared to the numbers recorded in 1990. This expanding rehabilitation need is largely unmet. In some lower-class countries, more than half of the people in need do

Talaa, S., El Fezazi, M., Jilbab, A., El yousfi Alaoui, M.H. (2023). Computer Vision-Based Approach for Automated Monitoring and Assessment of Gait Rehabilitation at Home. *International Journal of Online and Biomedical Engineering (iJOE)*, 19(18), pp. 139–157. https://doi.org/10.3991/ijoe.v19i18.43943

Article submitted 2023-08-09. Revision uploaded 2023-09-22. Final acceptance 2023-09-25.

© 2023 by the authors of this article. Published under CC-BY.

not receive sufficient rehabilitation care. Thus, the World Health Organization has launched the Rehabilitation 2030 initiative to address this rapidly enlarging unmet rehabilitation demand and relieve the difficulty among these people [2]. At-home rehabilitation offers the opportunity to address this need, especially when incorporating digital tools to facilitate and automate monitoring and exercise guidance. This allows individuals to receive timely feedback and support from healthcare professionals, even if they cannot physically be present.

In the context of gait rehabilitation, the knee joint angle is one of the main parameters to analyze biomechanical factors [3], identifying deficiencies or abnormalities, and guiding the development of targeted rehabilitation strategies [4]. Recently, motion capture (Mocap) systems have been increasingly adopted for gait analyzing equipment, offering enhanced precision in measuring joint angles. Generally, there are two types of MoCap systems: optical-based (marker or marker-less), and inertial sensors. The marker-based MoCap systems utilize cameras to track the movement of reflective markers attached to individuals. In the study by Ota et al. [5], the VICON system was proposed. These systems are known for their high accuracy in measuring human motion kinematics and are often considered the gold standard when compared to other motion capture (MoCap) systems. However, the marker-based MoCap system has notable disadvantages. It necessitates precise marker attachment and suitable lighting conditions. Additionally, it is limited by available space, can be expensive, and necessitates the use of markers. The imaging quality is also susceptible to variations caused by reflective objects and occlusion. In the studies cited in [6], [7], inertial measurement units (IMUs) were introduced. These are compact devices that can be attached to different body parts, including the feet, legs, and hips, to accurately measure movement and orientation. IMUs have the advantage of providing real-time feedback on gait patterns during rehabilitation, making them suitable for both clinical and home settings. However, it is important to note that IMUs can vary in cost, and higher-quality IMUs may be expensive, which can limit their accessibility for certain clinics or patients. Additionally, the utilization of IMUs requires specialized expertise in data analysis and interpretation, which may present a challenge in some settings.

Recently, there has been a growing interest in markerless-based systems, specifically pose-estimation algorithms. These algorithms utilize computer vision and deep neural networks to extract motion kinematics information accurately. This advancement presents new possibilities for the adoption of more effective methods for extracting MoCap data [8]. One example of these technologies is OpenPose, an open-source computer vision library. OpenPose utilizes deep neural networks to estimate the positions of human body joints, enabling the creation of 2D or 3D models of moving individuals [8]. In comparison to other MoCap systems mentioned earlier, this technique stands out as affordable and easy to set up, also a standard numerical camera can be used without special measurement equipment or environment [10]. This feature makes it suitable for simple integration and low-cost usage in home-based rehabilitation assessments. Video-based pose estimation has emerged as a valuable tool in the field of human gait rehabilitation, enabling the targeting of specific issues to enhance patients' quality of life. Numerous studies have focused on extracting human gait characteristics using pose estimation techniques. In [11], the author used the OpenPose approach to extract several gait parameters including joint angles. For instance, in a study referenced as [10], the authors utilized linear regression analysis to investigate the feasibility of estimating radiographic values from OpenPose measurements of knee angles in patients with knee osteoarthritis. This research aimed to enhance rehabilitation strategies for such patients. In another study referenced as [12], the authors compared spatiotemporal gait parameters, lower-limb sagittal plane joint kinematics, and condition-specific clinically relevant parameters. They simultaneously obtained data using 3D motion capture and sagittal and frontal plane videos. This comprehensive analysis was crucial in identifying and understanding specific deficits that need to be addressed before initiating treatment for gait rehabilitation. Additionally, a study mentioned as [13] emphasized the potential impact of measuring movement kinematics through pose estimation, specifically in post-stroke rehabilitation. The authors proposed interpreting clinically relevant movement parameters calculated using pose estimation, particularly based on OpenPose. This approach facilitated individualized care and improvements in post-stroke rehabilitation practices.

These studies collectively underscore the importance of utilizing pose estimation-based data acquisition in gait rehabilitation to facilitate targeted treatment strategies, personalized care, and improved rehabilitation outcomes. However, it is important to note that there are still limitations associated with these procedures. These limitations can be summarized as follows: 1) Determining specific features: There is a need to identify and extract precise features that provide comprehensive information about all phases of the gait cycle. This would enable a more detailed understanding of the patient's gait and guide treatment planning accordingly. 2) Limited comparative analysis: The procedures described in these studies primarily focused on comparing and monitoring the level of rehabilitation in patients. While this is valuable for tracking progress, it may be necessary to expand the scope of analysis to gain deeper insights into the effectiveness of different interventions and their impact on gait rehabilitation. Addressing these limitations could further enhance the utilization of pose estimation-based data acquisition in gait rehabilitation, enabling a more comprehensive understanding of gait dynamics and facilitating more effective and personalized treatment approaches.

In our study, we proposed a markerless-video based gait analysis system for automatic assessment of at-home rehabilitation. This system was able to deal with the abovementioned critical limitations. As noted, several studies have been conducted on this topic, but our methodology differs in many ways. First, we presented and validated the chosen pose estimation model in measuring knee angles during typical gait analyzing exercises. Secondly, after extracting critical gait cycle features, our aim was to calculate the rehabilitation score, which empowers both patients and healthcare providers with valuable insights. This scoring system leads to improved treatment strategies and better overall rehabilitation results. By quantifying the rehabilitation progress through the score, healthcare professionals can tailor interventions more effectively to each individual's needs and monitor their advancements over time. For patients, the rehabilitation score provides tangible feedback, fostering motivation and engagement in their recovery journey. Additionally, aggregated data from these scores can contribute to research, advancing our understanding of rehabilitation efficacy and optimizing outcomes for individuals with various gait-related challenges.

The remainder of this paper is structured as follows: In section 2, the methodology of the proposed approach and a general architecture is presented. In section 3, the results of the study are presented. Section 4, discusses the study's results is presented. While Section 5 provides a conclusion and outlines challenges for future studies.

2 METHODOLOGY

2.1 Overview

The workflow of the approach is illustrated in Figure 1. It consists of five processing steps. The first step is the video acquisition of the human gait using a low-cost camera. The second step is the pose estimation using the OpenPose framework, then the landmark coordinates extraction with a specific focus on the legs by correcting any incorrect estimations. In the third step, the extracted coordinates are utilized to determine the knee angles of the subjects, considering the hip, knee, and ankle coordinates. In the fourth and fifth steps, the resulting signal is used to extract seven features for each gait cycle. The sixth step and final one involved determining the rehabilitation score.

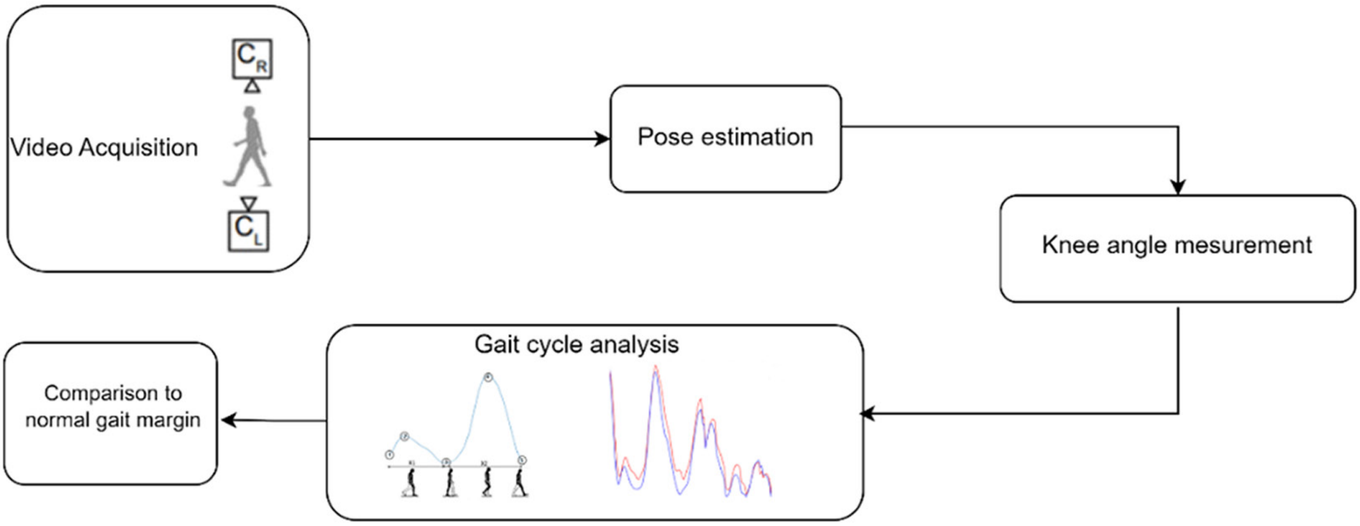

Fig. 1. Block diagram of processing steps

2.2 Computer vision-based knee angle estimation

Estimation of knee angles using computer vison method requires three main processes: pose estimation, landmarks coordinate extraction, relative angle calculation. Pose estimation is performed using OpenPose framework, a deep learning-based system that uses convolutional neural networks to estimate the pose of a person in the video [9], its architecture employed is illustrated in Figure 2. It utilized the Visual Geometry Group (VGG)-19 algorithm within OpenPose. Initially, the video clips were converted into frame-by-frame images and fed into the VGG-19 algorithm. After passing through the convolution and pooling layers of the VGG-19 algorithm, the images were transformed into a feature map (F). This feature map played a crucial role in identifying the specific joint under examination and established its connection to the corresponding individual depicted in the image. The feature map generated from the initial stage underwent a series of subsequent stages, with each stage comprising two branches. In Branch 1, the primary objective was to estimate the location of the joint and create a confidence map indicating the likelihood of its existence. Branch 2 was focused on estimating the part affinity fields (PAFs, denoted as 'L'), which determined the connections between joints based on these PAFs. The confidence map and PAFs obtained from the first stage were then used in the following stages to repeat the process and generate the skeleton representation. Through multiple stages and two branches, it estimated joint locations, created confidence maps, and calculated part affinity fields to generate the skeletal structure of the subjects and display an output JSON file representing the coordination landmarks results.

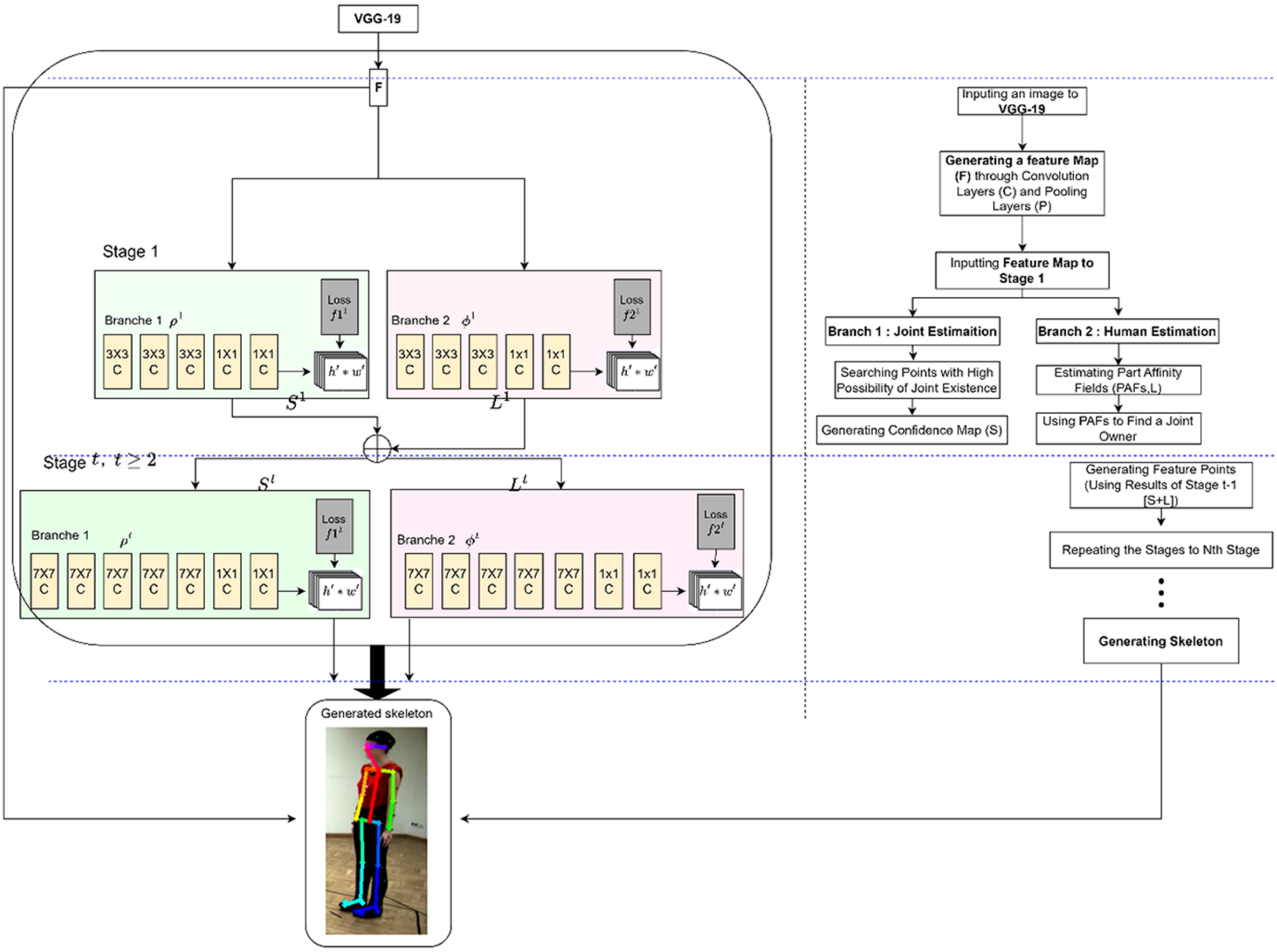

Fig. 2. OpenPose architecture

In previous research performed by the authors in [14], OpenPose was trained to generate three different poses with varying numbers of estimated key points: (a) MPI, the most basic model which can estimate 15 important key points, (b) the COCO model, a set of 18 points, and (c) the BODY_25 pose consisting of 25 key points. As shown in Figure 3, the MPI and COCO models include descriptors for the feet and pelvic center, while the BODY_25 pose model is the most detailed and is used in this study.

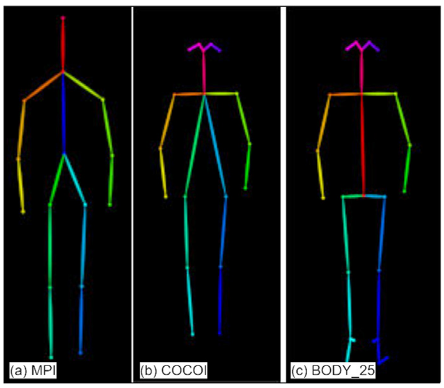

Fig. 3. OpenPose models: (a) MPI, (b) COCO, (c) Body_25

The extracted coordinates of the hip, knee, and ankle are used to calculate the knee angle using the vector product method. To measure the knee angles with the proposed approach, we followed the following steps.

First, a video of the subject has been obtained in the required posture, walking in sagittal from right to left or left to right, by ensuring that the video provides a clear view of the hip, knee, and ankle joints. Next, OpenPose is used to extract the coordinates of the hip, knee, and ankle joint centers from the video. The outputs are a video representing the pose estimation skeleton, and JSON files representing 2D coordinates of the key points. In the end, the (x–y) coordinates of the hip, knee, and ankle were used to calculate the knee angle θ_{Knee} (1) from the angles of the shank θ_{Shank} and thigh θ_{Thigh} showed in Figure 4. The equation is based on the fact that the knee joint is situated between the shank and thigh segments, and the angle at the knee can be calculated as the difference between the angles of these two segments [15]. The second equation, θ_{Shank} (2) is used to calculate the angle of the shank segment from the coordinates of the knee and ankle joint centers. The third equation, θ_{Thigh} (3) is used to calculate the angle of the thigh segment from the coordinates of the hip and knee joint centers. The measurements were repeated for each frame of the video to obtain a series of knee angles according to the frames.

$$\theta_{Knee} = \theta_{Shank} + (180 - \theta_{Thigh}) \tag{1}$$

$$\theta_{Shank} = tan^{-1}\left(\frac{y_{Knee} - y_{Ankel}}{x_{Knee} - x_{Ankel}}\right) \tag{2}$$

$$\theta_{Thing} = tan^{-1}\left(\frac{y_{Hip} - y_{Knee}}{x_{Hip} - x_{Knee}}\right) \tag{3}$$

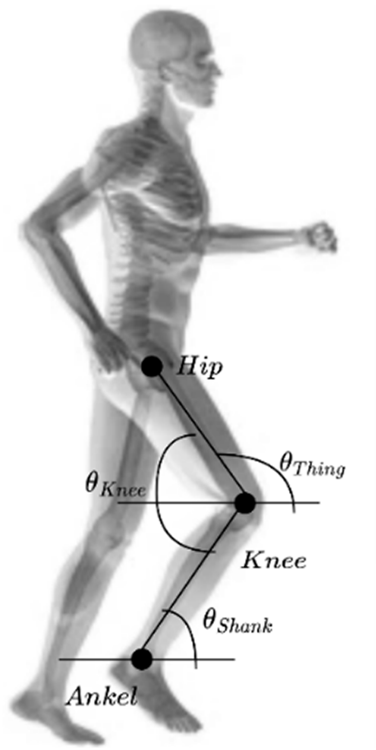

Fig. 4. Joint angles representation

2.3 Gait cycle analysis

The gait cycle refers to the sequence of events that occur during one complete stride or walking cycle Figure 5. It begins when one foot makes initial contact with the ground and ends when the same foot makes contact again. The gait cycle consists of two phases, the stance phase and the swing phase [16]. The stance phase begins when the foot makes initial contact with the ground and continues until the foot leaves the ground. It can be further divided into several events:

- Initial Contact: During this phase, there is a transfer of body weight towards the forward limb. The heel functions as a pivot point, allowing the knee to flex to absorb shock. Ankle plantar flexion further restricts the heel's rocking motion as the forefoot makes contact with the floor.
- Loading Response: The weight-bearing phase where the foot accepts the body's weight.
- Midstance: The point where the body's weight is directly over the foot.
- Terminal Stance: The period when the body moves forward over the foot.
- Pre-Swing: The transition phase as the foot prepares to leave the ground.

The swing phase, starts when the foot leaves the ground and ends when the foot makes initial contact again. It can be further divided into subphases:

- Initial Swing: The leg begins to move forward as the foot leaves the ground.
- Mid-Swing: In the second phase of the swing period, the limb is propelled forward through increased hip flexion, allowing the knee to extend naturally due to gravity. Simultaneously, the ankle continues dorsiflexing until it reaches a neutral position. This phase begins when the swinging limb aligns with the stance limb and concludes when the swinging limb is positioned forward with a vertical tibia, indicating an equilibrium between hip and knee flexion postures.
- Terminal Swing: The leg starts to slow down in preparation for the next stance phase.

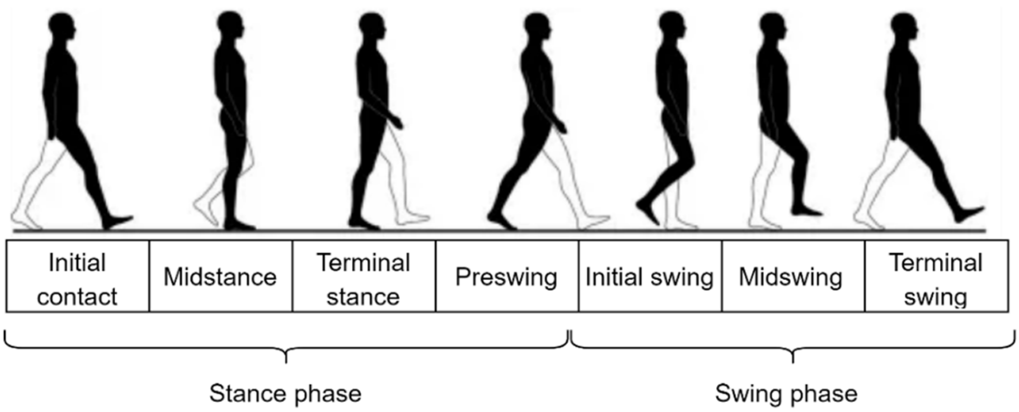

Fig. 5. Human gait cycle phases

To characterize the human gait from knee angles, five peaks and two times were identified as showing in Figure 6. These critical points corresponded to a one gait cycle. For instance, we determined the peak extension angle during the swing-to-stance phase, which represents the maximum extension of the knee as the leg transitions from swing to stance. Additionally, we identified the peak flexion angle during the loading response, indicating the maximum flexion of the knee as the foot makes contact with the ground. The peak extension angle in the terminal stance, peak flexion angle in the swing, and the peak of maximum knee extension adjacent to the heel strike were also determined, and ends by measuring the knee angle in the terminal swing.

To provide a comprehensive understanding of the gait cycle, we further calculated two times, the first one representing the time between the peak of the extension angle during the swing-to-stance phase and the peak extension angle in terminal stance, capturing the stance period, while the second denoted the time between the peak extension angle in terminal stance and the peak of the maximum knee extension adjacent to heel strike. This was in order to provide a comprehensive understanding of the gait cycle, indicating the swing period. These times provided crucial insights into the duration and timing of the stance and swing phases within the gait cycle.

By employing this approach, we can achieve a more precise and detailed characterization of the gait cycle, capturing the distinctive features and patterns exhibited by knee angles throughout the various phases.

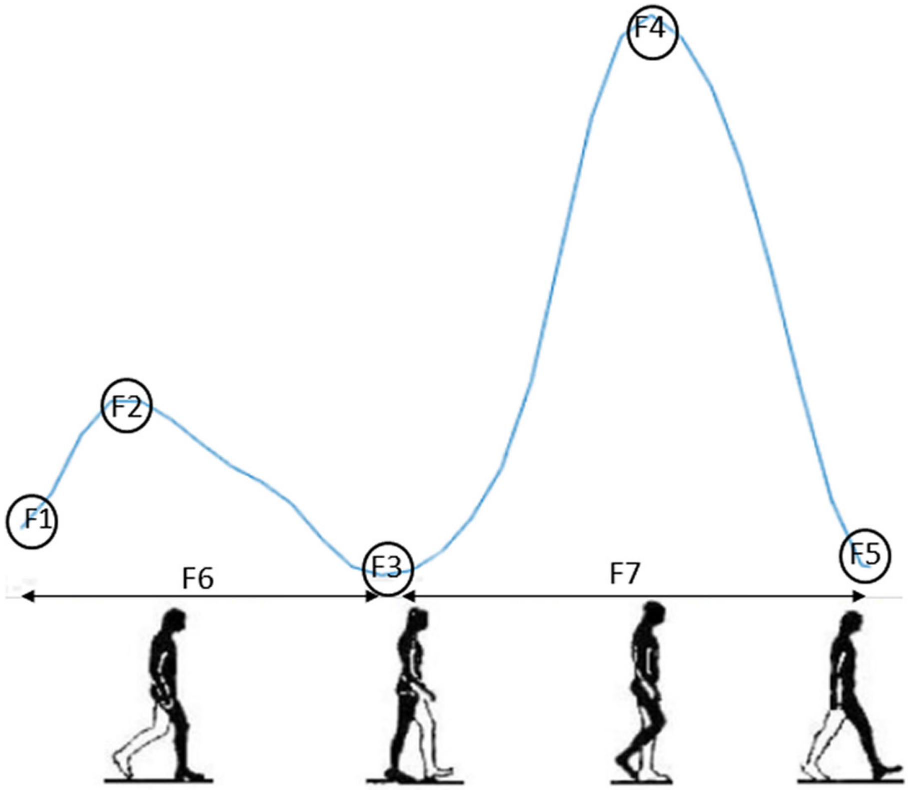

Fig. 6. The gait cycle features extracted, F1: extension angle in the swing to stance phase, F2: maximum knee flexion during stance phase, F3: maximum knee extension during terminal stance phase, F4: maximum knee flexion during the swing phase, and F5: maximum knee extension adjacent to heel strike. F6 and F7 are the difference time between F1–F3 and F3–F5

2.4 Rehabilitation assessment

In this study, we used the Dynamic Time Warping (DTW) algorithm to calculate the rehabilitation score of patients using the template data previously extracted.

The DTW algorithm was used to measure the similarity between two temporal sequences that may vary in speed or time [17]. It was originally developed for time series analysis and is widely used in recognizing similar patterns even if they occur at different speeds or time scales [18]. It is a powerful tool for time series analysis and pattern recognition tasks. The main idea behind DTW is to find the optimal alignment between two sequences, allowing for some local deformations in the time axis to find the best match. It takes into account both temporal shifts and amplitude variations between the sequences. The DTW algorithm [19] is presented below:

DTW Algorithm

Input: T: Template features, M: Measured features
Output: X: Optimal Time Warping Distance
Cost Matrix C shape (*n*+*1*, *m*+*1*);
Where n and m are the dimensions of the input vectors T and M;
p is the order of norm;
for *i*←*1* to *n* **do**
| C[*i*,*0*] ←∞;
end
for *i*←*1* to *n* **do**
| C[*0*,*i*] ←∞;
end
for *i*←*0* to *n*–*1* **do**
  for *j*←*0* to *m*–*1* **do**
   | C[*i*+*1*,*j*+*1*] ←| *T*[*i*] -*M*[*j*] |^p + min(C[*i*,*j*],C[*i*+*1*,*j*])
   end
end
return X

The final accumulated distance is the similarity score between the two sequences. Smaller distances indicate greater similarity, while larger distances imply more dissimilarity. Therefore, the DTW algorithm proved to be highly appropriate for identifying score rehabilitation.

The DTW distance is transformed into a range between 0 and 1 using the linearization and the min max normalization [20] methods, which employs the following equation (4):

$$X_{Norm} = \frac{X - X_{min}}{X_{max} - X_{min}} \tag{4}$$

Where X represents the measured distance for each feature, X_{min} is the minimum distance and the X_{max} is the maximum distance calculated.

As a result, the rehabilitation score (S_{Score}) can be calculated using the subsequent equation (5), standardized to a scale of 0 to 100 points. Lower percentages suggest an abnormal gait or an early stage of gait rehabilitation, whereas higher percentages indicate a normal gait.

$$S_{Score} = (1 - X_{Norm}) * 100 \tag{5}$$

2.5 Validation procedure

In this study, we validated the knee angle measurement using the publicly available GPJATK dataset [21]. This dataset comprises 166 data sequences involving

32 individuals walking normally. Each participant walked in a straight line over a known distance of 6.5 m from right to left (refer to Figure 7). The dataset comprises a motion capture (MoCap) database capturing three-dimensional movements and joint angles using 10 markers. The MoCap data was recorded using a VICON system consisting of 10 MX-T40 cameras, each with a resolution of 2352 × 1728 pixels, and a recording rate of 100 Hz. This specific portion of the GPJATK dataset serves as our reference.

Additionally, the dataset includes 2D video recordings obtained from four calibrated and synchronized video cameras. Each sequence's video data has a resolution of 960 × 540 pixels at a frame rate of 25 fps. We used the recordings captured by two cameras (C1 left and C3 right) to verify our proposed approach.

The synchronization between the video and motion capture data was achieved using VICON's MX-Giganet technology [21]. The output of the reference system was down-sampled to match the rate of the used cameras.

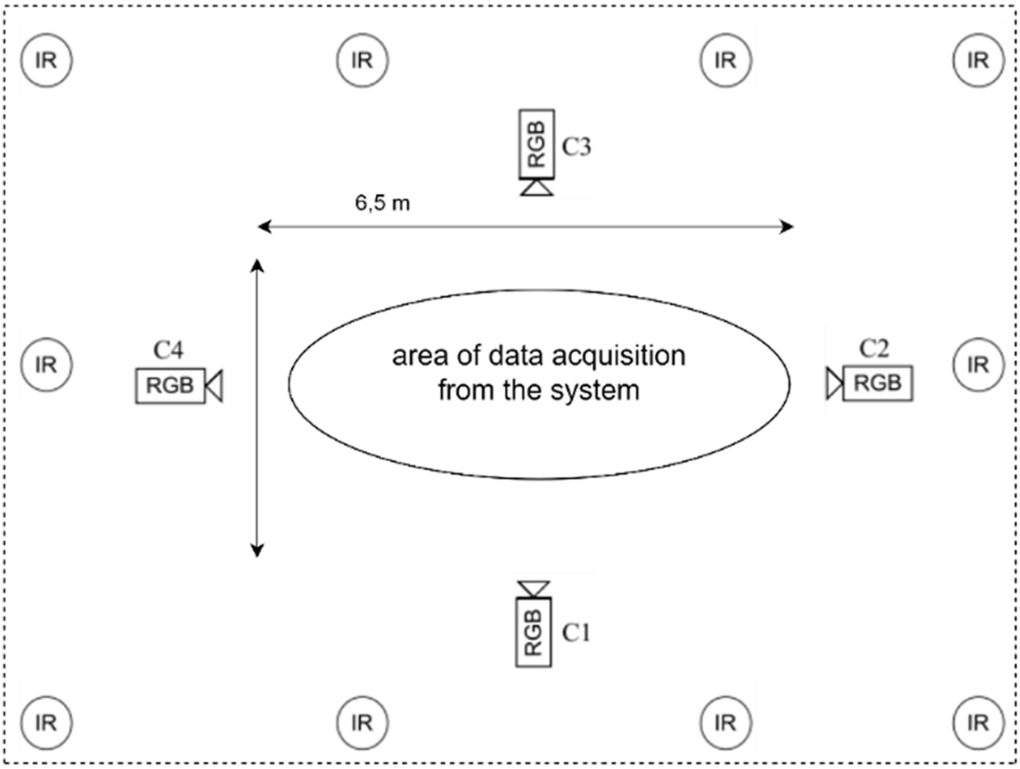

Fig. 7. Arrangement of data acquisition

To evaluate the accuracy of the measurements, we employed the Mean Absolute Error (MAE) [22]. Thus, the MAE represents the difference between the MoCap reference value obtained using the VICON system and the measured value acquired using the proposed markerless video-based method. The formula used for calculating the MAE is denoted as (6).

$$MAE = \frac{1}{n}\sum_{i=1}^{n}\left|x_i - \widehat{x_i}\right| \tag{6}$$

Where x_i is the reference, $\widehat{x_i}$ is the measured value, and n is the total number of data points.

The rest of the GPJATK dataset and another dataset of abnormal human gait in different levels of rehabilitation was taken from the Mission Gate dataset [23]. The videos format used is in mp4 with a frame rate of 30 fps:

- A1: Woman with a chronic hemiparetic gait.
- A2: Woman who suffers from gait dystonia (advanced rehabilitation level).
- A3: Man, with a gait against cerebral lesions.
- A4: Woman with multiple Sclerosis Gait.
- A5: Man, with a hemiplegic gait.
- A6: Man, with the gait of Parkinson's disease.

were used in the second part, which consist to calculate the rehabilitation score.

3 RESULTS

3.1 Knee angles validation

To validate the accuracy of the proposed approach, we compared the knee angles estimated using OpenPose for both cameras left (C1) and right (C3) to the reference angles obtained from the Vicon system. The qualitative evaluation of the compatibility between the estimated results and related references is shown in Figure 8. From these results, we can notice that the right knee angle estimated using both cameras (C1 and C3) showed that there is not much difference from the reference. As well as, for the left knee angle, the result obtained from both cameras (C1 and C3) showed that there is not much difference from the reference.

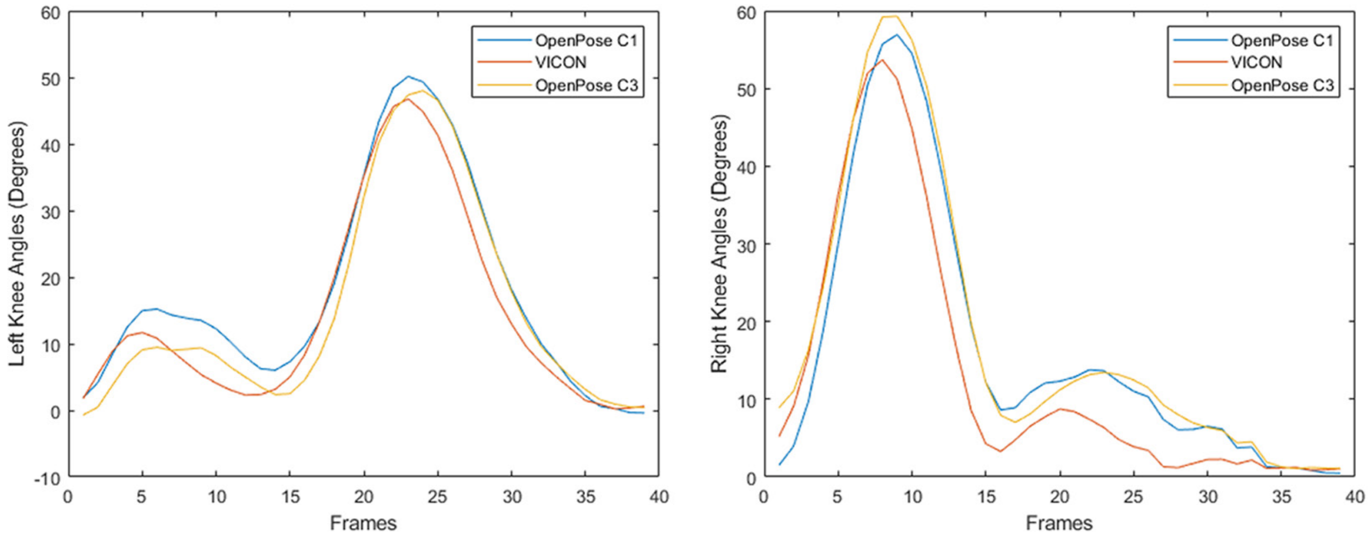

Fig. 8. Representation of knee angles throughout the gait cycle estimated using OpenPose for both cameras Left (C1) and Right (C3), and Vicon system

Table 1 illustrates MAE values between OpenPose and Vicon outputs for right and left knee angles sorted by the precise position of the camera. For the right knee, the C3-based angle demonstrated the minimal error (MAE = 5.74°) than the C1-based angle (MAE = 5.98°), with a difference of 0.24°. For the left knee, the C1-based angle presented the minimal error (MAE = 4.89°) than the C3-based angle (MAE = 5.24°), with a difference of 0.35°. These findings demonstrated acceptable accuracy, indicating the effectiveness of the proposed approach. Furthermore, these results highlight that the perspective of the participant relative to the camera viewpoints does not present a significant influence on the accuracy.

Table 1. Mean absolute error (MAE ± STD) of knee angles calculated using OpenPose and VICON system

Camera	Left Knee	Right Knee
Left c1	4.8951° ± 0.9697	5.9866° ± 1.2726
Right c3	5.2460° ± 1.8312	5.7432° ± 1.0507

3.2 Characterization of gait patterns

We have calculated the ranges and means of normal gait cycle features in a healthy population and presented the findings in Table 2. Additionally, we have differentiated between men and women to enhance precision. These results serve as a template for normal gait, which can be utilized to calculate the rehabilitation score and effectively assess and monitor the progress of individuals.

Table 2. Range and Mean ± STD of normal gait cycle features for men and women

Features	Range (Max–Min)		Mean	
	Men	Women	Men	Women
F1	9.15°	8.72	1.78° ± 3.35	1.71° ± 3.19
F2	10.51°	15.65°	16.47° ± 3.35	17.11° ± 4.67
F3	8.28°	11.39°	5.02° ± 3.12	4.98° ± 4.09
F4	10.11°	7.14°	65.5° ± 3.71	60.39° ± 2.7012
F5	10.4°	4.44°	–0.7° ± 3.19	1.37° ± 0.79
F6	7	2	13 ± 1.67	15 ± 1.22
F7	3	3	18 ± 3.46	18 ± 2.23

In Figure 9, we extracted the abnormal gait cycle features of individuals exhibiting various abnormal walking patterns. For women patients, in the case of (A1) with chronic hemiparetic gait, we observed increases of 10.55° in F2, 3.26° in F3, 18 in F6, and 3 in F7. Furthermore, there were gradual decreases of 0.99° in F1, 1.88° in F4, and 2.2° in F5 compared to the mean of normal gait cycles. For (A2) with gait dystonia, we observed increases of 3.18° in F3 and 2° in F7. Additionally, there were gradual decreases of 4.18° in F1, 4.58° in F2, 10.08° in F4, and 3.98° in F5 relative to normal. For (A4) with multiple sclerosis gait, we observed increases of 9.71° in F2, 13.46° in F3, 3.18° in F5, and 1° in F6. Furthermore, there were gradual decreases of 4.55° in F1, 4.1° in F4, and 7 in F7 compared to normal. For men patients, in the case of (A3) with gait against cerebral lesions, we observed increases of 11.84° in F1, 5.71° in F2, 15.07° in F3, 2 in F6, and 9 in F7. Furthermore, there were gradual decreases of 3.65° in F3 and 1.88° in F4 when compared to the mean of normal gait cycles. For (A5) with hemiplegic gait, we observed increases of 3.62° in F1 and 3.38° in F4. Furthermore, there were gradual decreases of 5.76° in F2, 3.92° in F3, 1.98° in F5, 1 in F6, and 2 in F7 compared to normal. For (A6) with Parkinson's disease gait, we observed increases of 5.6° in F2, 3.32° in F3, 1.59° in F5, and 9 in F6. Furthermore, there were gradual decreases of 1.24° in F1, 0.45° in F4, and 6 in F7 compared to normal.

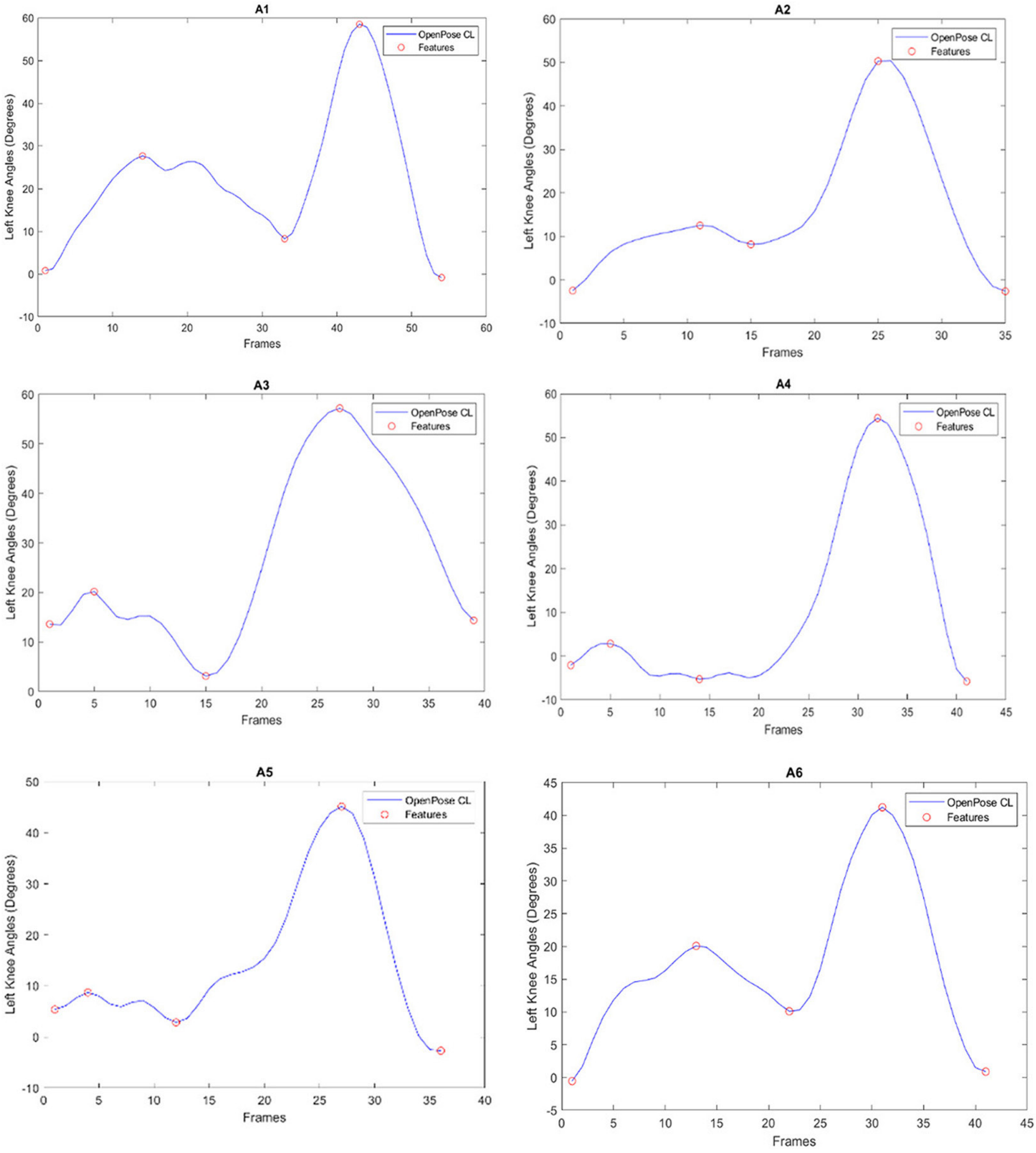

Fig. 9. Representation of abnormal gait cycles

A boxchart illustrating the distribution of extracted feature values in the gait cycle, comparing normal and abnormal gait, is presented in Figure 10. Upon initial observation, the distributions appear distinct. Notably, for men, a significant shift is observed at the levels of F4 and F7. Conversely, for women, a noticeable shift is observed at the levels of F1, F3, F4, F6 and F7.

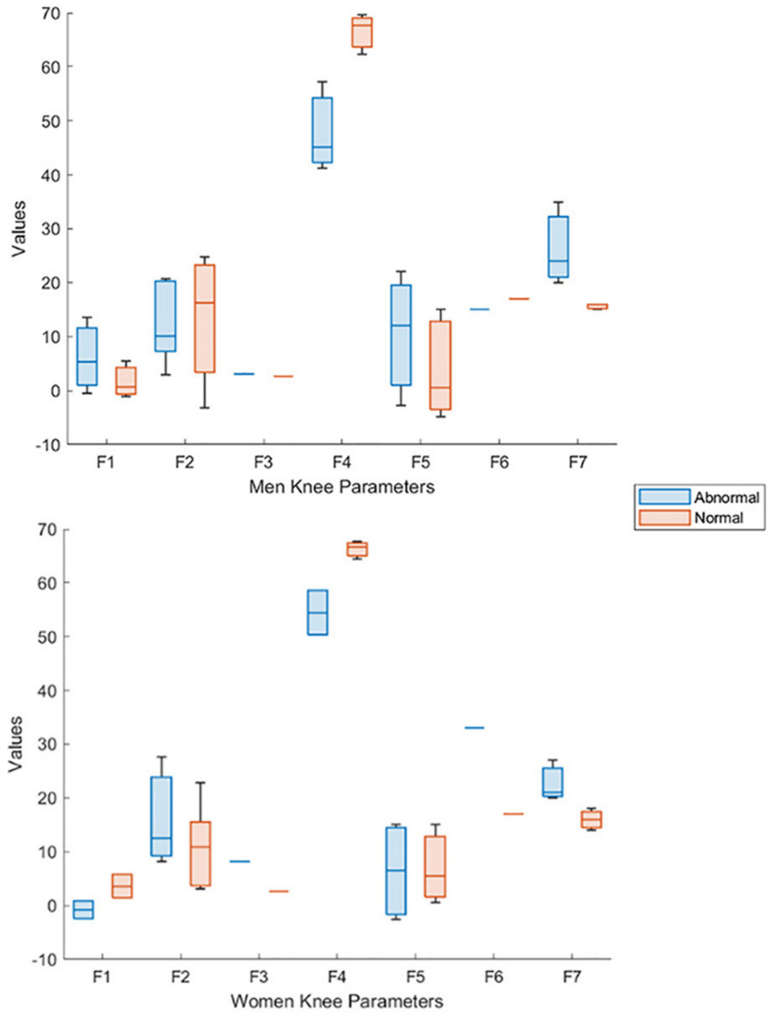

Fig. 10. Boxchart of extracted features in gait cycle for men and women

3.3 Rehabilitation score

In this part of the study, we aimed to calculate the rehabilitation score. The importance of a rehabilitation score for human gait lies in its ability to provide a quantitative assessment of a person's gait quality and rehabilitation progress.

As shown in Table 3, the calculated score values are very significant, allowing us to measure the rehabilitation score in normal gait with an average score of 97.8% and abnormal gait with an average score of 26.6%. For the subject W5, who is a woman who suffers from gait dystonia at an advanced rehabilitation level, we note that the score of 65% clearly shows this information. Lower percentages on the scale indicate the presence of an abnormal gait or the early stages of gait rehabilitation. This early identification of abnormalities or rehabilitation needs allows healthcare professionals to intervene promptly, tailor treatment plans, and address potential issues before they worsen. On the other hand, higher percentages suggest a more normalized gait, signifying successful rehabilitation and functional improvement. Such information is invaluable for patients, as it offers tangible feedback on their progress, instilling motivation and boosting confidence in their rehabilitation efforts. Additionally, healthcare providers can use these scores to monitor the effectiveness of interventions, compare outcomes among different patients, and optimize treatment strategies. Ultimately, the rehabilitation score plays a vital role in promoting better gait rehabilitation outcomes, enhancing patient care, and fostering an active and targeted approach to gait-related challenges.

Table 3. Rehabilitation score

	Subjects	Score
Normal	W1	97.5%
	W2	96.8%
	W3	100%
	M1	98.8%
	M2	100%
	M3	93.8%
Abnormal	W4	29%
	W5	65%
	W6	0%
	M4	0%
	M5	36%
	M6	30%

4 DISCUSSION

In this study, we presented a markerless video-based human gait analysis for automatic assessment of at-home rehabilitation. This approach relies on low-cost camera and deep learning algorithms. We measured the knee angles, and we extracted the specified features in a gait cycle, namely: (F1) extension angle in the swing to stance phase, (F2) maximum knee flexion during stance phase, (F3) maximum knee extension during terminal stance phase, (F4) maximum knee flexion during the swing phase, and (F5) maximum knee extension adjacent to heel strike, (F6) and (F7) are the time between (F1)–(F3) and (F3)–(F5). We evaluated the accuracy of the proposed approach against a marker pose estimation system (Vicon) using 2 cameras positioning, C1 for the left side and C3 for right side. Results demonstrate an acceptable accuracy between knee angles obtained from our markerless-based method and marker-based reference system. The accuracy of the measurements is not influenced by the position of the camera, as indicated in Table 1. Notably, when the camera is correctly positioned relative to the knee, the MAE observed is 3.3° for the left knee using both cameras C1 and C3, the MAE observed is less than 5° for the right knee using both cameras C1 and C3. That simplifies the use of the proposed approach at home without the need for specific camera and positioning.

These results were compared to previous studies focused on pose estimation approaches using the OpenPose framework. For instance, Jan Stenum et al. [11] reported an average MAE of 3.5° for the knee joint angle in the sagittal plane compared to marker-based method. In another study in [10], the authors evaluated the accuracy of OpenPose in estimating sagittal plane knee joint angle by comparing it with the marker-based method. The study reported MAE values of 5.1° for the left knee and 5.6° for the right knee using the left camera. Furthermore, when utilizing the right camera, the MAE values were found to be 5.5° for the left knee and 5.6° for the right knee.

After validating the accuracy of the proposed approach, we proceeded to measure the mean values of the features for subjects with normal gait. These mean values would serve as a template to define the gait rehabilitation score. We employed the DTW algorithm to calculate the time between two sequences: the mean values of features in normal gait and the measured features of the subject undergoing rehabilitation. The resulting time was converted to a percentage using equation (6), providing a meaningful value. A percentage close to 100% indicates a normal gait, while 0% signifies an abnormal gait prior to rehabilitation. To validate this equation, we tested it on individuals with normal gait and observed high scores around 93.8% to 100%. In subjects with abnormal gait, lower scores were obtained, ranging from 0% to 36%. Additionally, we evaluated a critical case involving a subject at an advanced stage of rehabilitation, which resulted in a score of 65%. These scores demonstrate the efficacy of our approach in assessing rehabilitation progress and distinguishing between normal and abnormal gait patterns.

While our approach offers promising advantages in gait rehabilitation monitoring, it is important to acknowledge its limitations. One significant limitation lies in the database used for validation. The accuracy and reliability of results heavily depend on the quality and diversity of the data within the database. If the dataset is limited in size or lacks representation from various gait patterns, it may impact the generalizability and robustness of our approach to different populations or scenarios. Additionally, an investigation into background clutter colors is another crucial aspect to consider. The presence of complex and varying backgrounds could potentially interfere with the accuracy of pose estimation algorithms, leading to errors in gait analysis. To mitigate this influence on accuracy, further research and refinement of our approach are needed. Overall, addressing these limitations will be essential for enhancing the effectiveness and applicability of our gait analysis system in real-world settings.

In conclusion, our approach demonstrates acceptable accuracy in measuring knee joint angles during a sagittal walk and provides a quantitative rehabilitation score. Moreover, our video-based approach proves to be highly portable and cost-effective compared to other motion capture (MoCap) systems. As a result, it presents a viable alternative for automatically monitoring home-based rehabilitation progress, providing a convenient and accessible solution for patients.

5 CONCLUSION

In this study, we presented a markerless video-based human gait analysis system for automatic assessment of at-home rehabilitation. Our approach relies on low-cost cameras and deep learning algorithms to measure knee angles and extract specified gait cycle features. The accuracy of our method was evaluated against a marker-based reference system, and the results demonstrated an acceptable accuracy for knee angle measurements. Notably, the accuracy was not influenced by the camera's position, making the system easy to use at home without specific camera requirements.

We also introduced a gait rehabilitation score that utilizes the DTW algorithm to measure the time between normal gait features and the subject's measured features. The resulting percentage-based score effectively distinguishes between normal and abnormal gait patterns and provides valuable insights into the individual's rehabilitation progress.

Despite its advantages, we acknowledge some limitations in our approach. The quality and diversity of the validation database may affect the generalizability of results, highlighting the need for more extensive datasets. Additionally, we identified potential challenges related to background clutter colors that could influence pose estimation accuracy, warranting further research and refinements. In conclusion, our markerless video-based gait analysis system offers accurate measurements and provides a valuable rehabilitation score for monitoring progress. Its portability and cost-effectiveness make it a viable alternative for automatic at-home rehabilitation assessment. By addressing the identified limitations, our approach holds great promise for enhancing gait analysis and improving rehabilitation outcomes in real-world settings.

6 REFERENCES

[1] Cieza, Alarcos, Causey, Kate, Kamenov, Kaloyan, *et al.,* "Global estimates of the need for rehabilitation based on the global burden of disease study 2019: A systematic analysis for the global burden of disease study 2019," *The Lancet,* vol. 396, no. 10267, pp. 2006–2017, 2020. https://doi.org/10.1016/S0140-6736(20)32340-0

[2] G.W.H., "Organization, Rehabilitation 2030 initiative," 2017. https://www.who.int/initiatives/rehabilitation-2030

[3] Astudillo, Alejandro, Avella-Rodríguez, Edna, Arango-Hoyos, Gloria, *et al.,* "Smartphone-based wearable gait monitoring system using wireless inertial sensors," *International Journal of Online & Biomedical Engineering*, vol. 19, no. 8, pp. 38–55, 2023. https://doi.org/10.3991/ijoe.v19i08.38781

[4] De Miguel-Fernández, Jesús, Lobo-Prat, Joan, Prinsen, Erik, *et al.*, "Control strategies used in lower limb exoskeletons for gait rehabilitation after brain injury: A systematic review and analysis of clinical effectiveness," *Journal of Neuroengineering and Rehabilitation*, vol. 20, no. 1, p. 23, 2023.

[5] Ota, Megumi, Tateuchi, Hiroshige, Hashiguchi, Takaya, *et al.,* "Verification of validity of gait analysis systems during treadmill walking and running using human pose tracking algorithm," *Gait & Posture*, vol. 85, pp. 290–297, 2021. https://doi.org/10.1016/j.gaitpost.2021.02.006

[6] Gu, Chenyu, Lin, Weicong, He, Xinyi, *et al.*, "IMU-based Mocap system for rehabilitation applications: A systematic review," *Biomimetic Intelligence and Robotics*, vol. 3, no. 2, p. 100097, 2023. https://doi.org/10.1016/j.birob.2023.100097

[7] El Fezazi, Mohamed, Achmamad, Abdelouahad, Jbari, Atman, *et al.,* "A convenient approach for knee kinematics assessment using wearable inertial sensors during home-based rehabilitation: Validation with an optoelectronic system," *Scientific African*, vol. 20, p. e01676, 2023. https://doi.org/10.1016/j.sciaf.2023.e01676

[8] Moro, Matteo, Marchesi, Giorgia, Hesse, Filip, *et al.,* "Markerless vs. marker-based gait analysis: A proof of concept study," *Sensors*, vol. 22, no. 5, p. 2011, 2022. https://doi.org/10.3390/s22052011

[9] Lee, Bogyeong, Hong, Sungkook, and Kim, Hyunsoo, "Determination of workers' compliance to safety regulations using a spatio-temporal graph convolution network," *Advanced Engineering Informatics*, vol. 56, p. 101942, 2023. https://doi.org/10.1016/j.aei.2023.101942

[10] Saiki, Yoshitomo, Kabata, Tamon, Ojima, Tomohiro, *et al.,* "Reliability and validity of OpenPose for measuring hip-knee-ankle angle in patients with knee osteoarthritis," *Scientific Reports*, vol. 13, no. 1, p. 3297, 2023. https://doi.org/10.1038/s41598-023-30352-1

[11] Stenum, Jan, Rossi, Cristina, and Roemmich, Ryan T., "Two-dimensional video-based analysis of human gait using pose estimation," *PLoS Computational Biology*, vol. 17, no. 4, p. e1008935, 2021. https://doi.org/10.1371/journal.pcbi.1008935

[12] Stenum, Jan, Hsu, Melody, Pantelyat, Alexander, *et al.,* "Clinical gait analysis using video-based pose estimation: Multiple perspectives, clinical populations, and measuring change," *MedRxiv*, p. 2023.01.26.23285007, 2023. https://doi.org/10.1101/2023.01.26.23285007

[13] Guo, Liquan, Zhang, Bochao, Wang, Jiping, *et al.,* "Wearable intelligent machine learning rehabilitation assessment for stroke patients compared with clinician assessment," *Journal of Clinical Medicine*, vol. 11, no. 24, p. 7467, 2022. https://doi.org/10.3390/jcm11247467

[14] Zhang, Frederick, Juneau, Pascale, Mcguirk, Connor, *et al.,* "Comparison of OpenPose and HyperPose artificial intelligence models for analysis of hand-held smartphone videos," in *2021 IEEE International Symposium on Medical Measurements and Applications (MeMeA)*, IEEE, 2021, pp. 1–6. https://doi.org/10.1109/MeMeA52024.2021.9478740

[15] El Fezazi, Mohamed, Jbari, Atman, and Jilbab, Abdelilah, "Conceptual architecture of AI-Enabled IoT system for knee rehabilitation exercises telemonitoring," in *Artificial Intelligence and Industrial Applications: Artificial Intelligence Techniques for Cyber-Physical, Digital Twin Systems and Engineering Applications*, Springer International Publishing, 2021, pp. 200–209. https://doi.org/10.1007/978-3-030-53970-2_19

[16] Haider, Saif M. J., Takhakh, Ayad M., Al-Waily, Muhannad, *et al.,* "Simulation of gait cycle in sagittal plane for above-knee prosthesis," in *AIP Conference Proceedings*, AIP Publishing, 2022. https://doi.org/10.1063/5.0066819

[17] Omerovic, Ajdin. Time series classification, 2022.

[18] Prasetio, Barlian Henryranu and Syauqy, Dahnial, "Design of speaker verification using dynamic time warping (DTW) on graphical programming for authentication process," *Journal of Information Technology and Computer Science*, vol. 2, no. 1, pp. 11–18, 2017. https://doi.org/10.25126/jitecs.20172124

[19] Fu, Tak-chung, "A review on time series data mining," *Engineering Applications of Artificial Intelligence*, vol. 24, no. 1, pp. 164–181, 2011. https://doi.org/10.1016/j.engappai.2010.09.007

[20] Jahan, Ali and Edwards, Kevin L., "A state-of-the-art survey on the influence of normalization techniques in ranking: Improving the materials selection process in engineering design," *Materials & Design (1980–2015)*, vol. 65, pp. 335–342, 2015. https://doi.org/10.1016/j.matdes.2014.09.022

[21] Kwolek, Bogdan, Michalczuk, Agnieszka, Krzeszowski, Tomasz, *et al.,* "Calibrated and synchronized multi-view video and motion capture dataset for evaluation of gait recognition," *Multimedia Tools and Applications*, vol. 78, pp. 32437–32465, 2019. https://doi.org/10.1007/s11042-019-07945-y

[22] Hodson, Timothy O., "Root-mean-square error (RMSE) or mean absolute error (MAE): When to use them or not," *Geoscientific Model Development*, vol. 15, no. 14, pp. 5481–5487, 2022. https://doi.org/10.5194/gmd-15-5481-2022

[23] Harrell, Irvin B., *et al.,* "College of Health Sciences Newsletter," September 2017.

7 AUTHORS

Safae Talaa received her master's degree in Genie Electrical Engineering at the University of Mohammed V, ENSAM Rabat, Morocco, in 2022. She is a PhD student of science and technology of the engineer in ENSIAS, researcher in Artificial Intelligence applied to biomedical engineering. Her research interest includes human gait analysis and diagnosis based on AI and IOT applications. She is part of the Team E2SN – Biomedical Engineering Research Laboratory ENSAM-Rabat (E-mail: safae_talaa@um5.ac.ma).

Mohamed El Fezazi received his master's degree in Electrical Engineering from the High School of Technical Education (ENSET) Rabat Mohammed V University, Morocco, in 2018. Currently PhD student with Electronic Systems, Sensors and Nano biotechnologies (E2SN) Research Team at ENSAM, Mohammed V University in Rabat, Morocco. His interests are in Biomedical Signal Processing and Internet of Medical Things (IoMT) (E-mail: elfezazi.med@gmail.com).

Abdelilah Jilbab Professor of Electrical Engineering at ENSAM Rabat of the University of Mohammed V in Rabat. He acquired his PhD. in Computer and Telecommunication from the Mohammed V Agdal University, Rabat, Morocco in February 2009. He has published in the field of image processing, sensor networks, and signal processing for Parkinson's disease. His current interest is in embedded systems and wireless sensor networks (WSN) applied to biomedical. Dr. Jilbab is a member of the research laboratory E2SN – Biomedical Engineering Research Laboratory at ENSAM-Rabat at Mohamed V University (E-mail: a.jilbab@um5r.ac.ma).

My Hachem El Yousfi Alaoui Professor of Biomedical Engineering at the University of Mohammed V, ENSAM-Rabat, is a member of the researcher laboratory E2SN – Biomedical Engineering Research Laboratory at ENSAMRabat, Mohamed V University in Rabat, Morocco. A member of the E2SN research group, Prof. EL yousfi's current research work is focused on biomedical data processing, AI, IoT and the hardware implementation of associated circuits (E-mail: h.elyousfi@um5r.ac.ma).